Spatial localization of intense high-frequency fields in a plasma that is parametrically unstable in the lower hybrid resonance region

S. N. Gromov, L. L. Pasechnik, and V. F. Semenyuk

Institute of Nuclear Research, Ukrainian Academy of Sciences
(Submitted March 21, 1976)
Pis'ma Zh. Eksp. Teor. Fiz. **23**, No. 9, 509–512 (5 May 1976)

Sharply localized intense radio-frequency (RF) fields were observed with the aid of a probing electron beam in a magnetized plasma during the nonlinear stage of the modulation instability of electron plasma waves with dispersion $\omega = \omega_{pe}(k_\parallel / k)$. The characteristic amplitudes and the spatial scales of these fields, the appearance of which is attributed to collapse of plasma waves, are estimated.

PACS numbers: 52.35.En

During the nonlinear stage of modulation instability of Langmuir waves, collapse[1] gives rise to regions of localization of strong RF fields. The present paper is devoted to a search for such regions in a magnetized plasma, in which modulation instability of plasma waves was parametrically excited in the region of the lower hybrid resonance, and with a dispersion $\omega = \omega_{pe}(k_\parallel/k)$ (ω_{pe} is the electron plasma frequency).

The plasma was produced in a dielectric tube 60 cm long and 6 cm in diameter by a spatially-periodic RF field. The pump frequency was $f_0 = 21$ MHz, the density n_e and temperature T_e of the plasma electrons were in the ranges $n_e = (0.2—2) \times 10^9$ cm^{-3} and $T_e = (8—25)$ eV, the magnetic field intensity was $H = 850$ Oe, and the pressure of the working gas (helium) was $\sim 10^{-3}$ mm Hg. The longitudinal and transverse components of the intensity and of the wave vector of the pump wave satisfied the relation $E_{0\parallel}/E_{0\perp} \approx k_{0\parallel}/k_{0\perp} \approx 0.1$. The values at the instability threshold were $E_{0\parallel} \approx 1$ V/cm and $k_{0\parallel} \approx 0.3$ cm^{-1}.

The low-frequency plasma-density modulation, which is a characteristic of the modulation instability, reached 15% at $E_0 \approx 3E_{0\,\mathrm{thr}}$, and the spatial structure of the oscillations, which was clearly pronounced at $E_0 \sim E_{0\,\mathrm{thr}}$ then became fully randomized, thus indicating enrichment of the oscillations with components having larger k. The linear characteristics of this instability are described in[2].

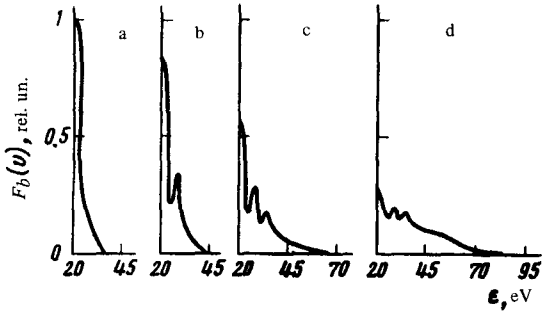

FIG. 1. Distribution function of probing electron beam for different pump-field amplitudes and different beam ranges L: a) $E_0 < E_{0\,\mathrm{thr}}$, $L = 30$ cm; b) $E_0 \approx 3E_{0\,\mathrm{thr}}$, $L = 6$ cm, c) $E_0 \approx 3E_{0\,\mathrm{thr}}$, $L = 14$ cm; d) $E_0 \approx 3E_{0\,\mathrm{thr}}$, $L = 23$ cm.

The RF electric fields produced in the plasma upon development of the modulation instability were investigated with a probing electron beam by a method in which the energy spectrum and the radial broadening of a weak (producing no effects whatever) electron beam are analyzed. The probing beam, of ~ 1 cm diam, was produced by a thermionic cathode placed on the system axis in the region of the homogeneous plasma. The beam current ranged from 50 to 250 μA and the energy from 20 to 100 eV. Use of low-frequency (33 Hz) modulation of the cathode heater current made it possible to separate readily the beam electrons from the background of the plasma electrons even at a ratio $n_b/n_e < 10^3$ (n_b is the electron density in the beam). The beam characteristics were measured with a movable multigrid electrostatic analyzer.

Figures 1b, 1c, and 1d show the distribution functions $F_b(v)$ of the beam electrons of energy $\mathcal{E} = 20$ eV with respect to the longitudinal velocity component at different distances from the cathode, under conditions of advanced instability ($E_0 \approx 3E_{0\,\mathrm{thr}}$). It is seen that when the beam range is increased $F_b(v)$, not only broadens but acquires first one peak and then two equidistant peaks, which become smoothed out at large ranges. In the absence of instability (Fig. 1a), the form of $F_b(v)$ is practically independent of the range of the beam, and is apparently determined by the velocity spread of the electrons in the space-charge layer surrounding the cathode. The distance between peaks is proportional to the pump field intensity and independent of the initial beam energy.

The deformation of the distribution function of the probing beam is accompanied, as seen from Fig. 2, by an appreciable broadening of the beam, proportional to the pump-field intensity. The beam broadening is also proportional to the beam range in the plasma. At $E_0 < E_{0\,\mathrm{thr}}$, the radial distributions of the beam at different ranges practically coincide and are close to that shown by curve 1 of Fig. 2.

The effects described above manifest themselves to the fullest degree at low initial beam energies $\mathcal{E} \sim T_e$. They become less pronounced with increasing energy and vanish at $\mathcal{E} \sim (4-5)T_e$.

We emphasize that the observed phenomena cannot be connected with the beam-plasma interaction, since neither the form of the distribution function no

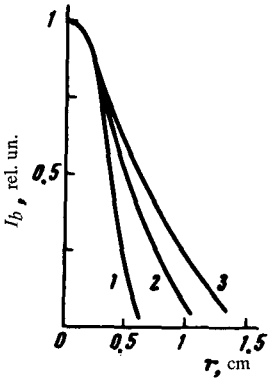

FIG. 2. Radial distribution of the beam current for different pump field amplitudes: $\mathcal{E}=20$ eV, $L=30$ cm; 1) $E_0 < E_{0\,\mathrm{thr}}$, 2) $E_0 \approx 2E_{0\,\mathrm{thr}}$, 3) $E_0 \approx 3E_{0\,\mathrm{thr}}$.

he beam broadening depends on the beam current in the working range of currents.

All the observed effects can be unambiguously explained if there exist in the plasma regions of localization of strong RF electric fields—caverns. Recent numerical experiments[3] show that the appearance of such regions is possible as a result of collapse of the plasma waves also in the region of the lower hybrid resonance. Then the peaks in the distribution function are due to the interaction of the electrons with the longitudinal cavern field $E_{\parallel}$, and the broadening of the beam is attributed to the drift of the electrons under the influence of the transverse component $E_{\perp}$ of the cavern field.

Figures 3a and 3b show the results of a numerical experiment that simulates the passage of a monoenergetic beam with $\mathcal{E}=20$ eV in succession through one cavern (Fig. 3a) and then through another (Fig. 3b). Some 85% of the beam particles pass through each cavern. We have considered the simplest case when the longitudinal field component $E=E_{\parallel}\cos(\omega_0 t+\phi)$ is constant along the cavern, the phases ϕ of the particles entering the cavern have a uniform distribution from zero to 2π, $E_{\parallel}=7.5$ V/cm, and the cavern length is $l_{\parallel}=1.33$ cm. It is seen that passage through each successive cavern is accompanied by the appearance of a new peak on the distribution function $F_b(v)$, the distance between peaks being

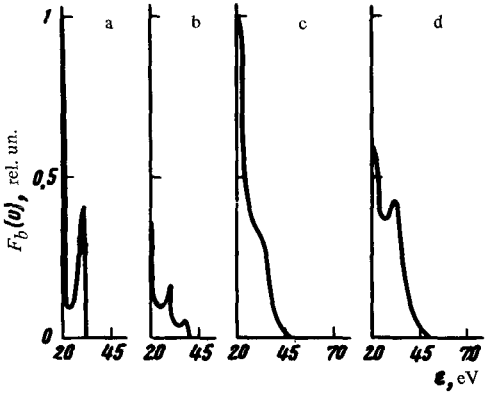

FIG. 3. Electron-beam distribution functions obtained by numerical simulation.

$\Delta\mathcal{E} \approx E_{\parallel} l_{\parallel}$. Figures 3c and 3d illustrate the passage of a beam with an experimentally obtained distribution function through one such cavern. The peak appears on the distribution function when $Q = 80\%$ of the beam electrons interact with the cavern (Fig. 3d). A value $Q = 60\%$ turns out to be insufficient even for the appearance of the first peak. (Fig. 3c).

Within the framework of the indicated concepts, it is easy to explain such experimental facts as the equal distances between the peaks, the increase of $\Delta\mathcal{E}$ with increasing pump field, and the independence of $\Delta\mathcal{E}$ of the initial energy of the probing electrons.

Let us estimate the characteristic fields and the spatial scales of the resultant caverns. The estimates given below are for a pump field amplitude $E_0 \approx 30$ V/cm that is three times larger than the threshold of the modulation instability.

Knowing the density modulation depth $\delta n/n \approx 10\%$, we determined the field in the cavern from the relation $E^2/16\pi n_e T_e \approx \delta n/n$, $E^2 = E_{\parallel}^2 + E_{\perp}^2$. Assuming that $E_{\parallel} \ll E_{\perp}$ in the cavern just as in the initial wave, we find that at $n_e \approx 2 \times 10^9$ cm^{-3} and $T_e \approx 20$ eV we have $E \approx E_{\perp} \approx 160$ V/cm. From the value of the field $E_{\perp}$, which determines the transverse beam-electron drift velocity, and from the beam broadening $\Delta R \approx 0.25$ cm, we can determine the sum $Nl_{\parallel}$ of the longitudinal cavern lengths, which turns out to be ~ 4 cm.

Since the first peak on the beam distribution function is registered already at a distance 5 cm from the cathode, it follows that at a range of 30 cm the beam passes through $N = 6$ caverns. Therefore $l_{\parallel} \approx 0.7$ cm and from the distance between the peaks of the fine structure we get $E_{\parallel} \approx \Delta\mathcal{E}/l_{\parallel} = 15$ V/cm.

The fact that the distribution function $F_b(v)$ has a fine structure only when the beam energy is low can be attributed to the increase, at low velocities, in the number of particles that pass through the cavern region with maximal field. This allows us to assume that the transverse dimension $l_{\perp}$ of the cavern is of the order of the drift distance of the slow electron in the field of one cavern, and amounts to $l_{\perp} \approx 0.05 \pm 0.1$ cm.

Thus, the caverns are ellipsoidal formations elongated along the magnetic field with scales approximately 1/20th of the corresponding dimensions of the pump wave, and with an RF field intensity approximately five times larger than the pump-field amplitude.

[1]T.A. Gorbushina, L.M. Detryarev, V.E. Zakharov, and V.N. Ravinskaya, Preprint IPM No. 128, Moscow, 1975.
[2]L.L. Pasechnik and V.F. Semenyuk, Zh. Tekh. Fiz. **45**, 779 (1975) [Sov. Phys. Tech. Phys. **20**, 491].
[3]S.L. Musher and B.I. Sturman, Pis'ma Zh. Eksp. Teor. Fiz. **22**, 537 (1975) [JETP Lett. **22**, 265 (1975)].